AD-A146 094 A STUDY OF THE CRITICAL LAYER IN A ROTATING LIQUID 1/1
PAYLOAD(U) ARMY ARMAMENT RESEARCH AND DEVELOPMENT
CENTER ABERDEEN PROVIN.. R SEDNEY ET AL. AUG 84
UNCLASSIFIED ARBRL-TR-02582 SBI-AD-F300 478 F/G 19/6 NL

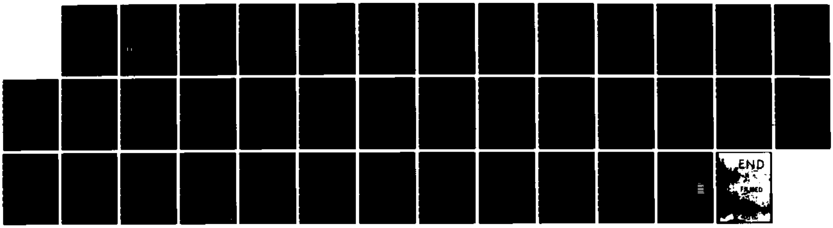

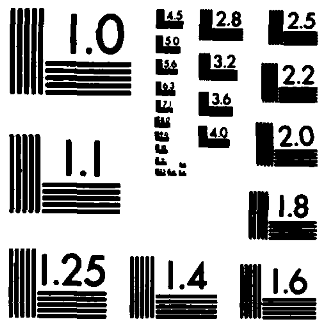

MICROCOPY RESOLUTION TEST CHART
NATIONAL BUREAU OF STANDARDS-1963-A

(12)

AD

TECHNICAL REPORT ARBRL-TR-02582

A STUDY OF THE CRITICAL LAYER IN A ROTATING LIQUID PAYLOAD

AD-A146 094

Raymond Sedney
Nathan Gerber

August 1984

US ARMY ARMAMENT RESEARCH AND DEVELOPMENT CENTER
BALLISTIC RESEARCH LABORATORY
ABERDEEN PROVING GROUND, MARYLAND

UNCLASSIFIED
SECURITY CLASSIFICATION OF THIS PAGE (When Data Entered)

REPORT DOCUMENTATION PAGE		READ INSTRUCTIONS BEFORE COMPLETING FORM
1. REPORT NUMBER TECHNICAL REPORT ARBRL-TR-02582	2. GOVT ACCESSION NO. ADA146094	3. RECIPIENT'S CATALOG NUMBER
4. TITLE (and Subtitle) A STUDY OF THE CRITICAL LAYER IN A ROTATING LIQUID PAYLOAD		5. TYPE OF REPORT & PERIOD COVERED Final
		6. PERFORMING ORG. REPORT NUMBER
7. AUTHOR(s) Raymond Sedney Nathan Gerber		8. CONTRACT OR GRANT NUMBER(s)
9. PERFORMING ORGANIZATION NAME AND ADDRESS US Army Ballistic Research Laboratory ATTN: DRXBR-LFD Aberdeen Proving Ground, Maryland 21005-5066		10. PROGRAM ELEMENT, PROJECT, TASK AREA & WORK UNIT NUMBERS RDT&E 1L161102AH43
11. CONTROLLING OFFICE NAME AND ADDRESS US Army Ballistic Research Laboratory ATTN: DRXBR-OD-ST Aberdeen Proving Ground, Maryland 21005-5066		12. REPORT DATE August 1984
		13. NUMBER OF PAGES 37
14. MONITORING AGENCY NAME & ADDRESS(if different from Controlling Office)		15. SECURITY CLASS. (of this report) Unclassified
		15a. DECLASSIFICATION/DOWNGRADING SCHEDULE

16. DISTRIBUTION STATEMENT (of this Report)

Approved for public release; distribution unlimited.

17. DISTRIBUTION STATEMENT (of the abstract entered in Block 20, if different from Report)

18. SUPPLEMENTARY NOTES

19. KEY WORDS (Continue on reverse side if necessary and identify by block number)

Critical Layer
Eigenvalue Problem - Rotating Flow
Liquid-Filled Projectile
Rotating Fluid
Spin-Up

20. ABSTRACT (Continue on reverse side if necessary and identify by block number) (bja)

The unsteady motion of a fluid which fills a spinning cylinder is considered. Spin-up of the fluid is the basic flow which is perturbed. Non-axisymmetric, viscous perturbations are used to study the wave motion and critical layer. The frequencies and decay rates are determined by the eigenvalues of the system of perturbation equations. For large time the fluid

(continued)

DD FORM 1 JAN 73 1473 EDITION OF 1 NOV 65 IS OBSOLETE

UNCLASSIFIED
SECURITY CLASSIFICATION OF THIS PAGE (When Data Entered)

approaches solid body rotation; for this state there is no critical layer and the eigenvalue problem is considerably simpler. The critical layer always exists for small time; it ceases to exist at a time which depends on the parameters of the basic flow and the wave motion. Time histories of the eigenvalues and of the critical layer are given for two cases and two radial modes. The effects of the critical layer on the eigenfunctions and the phase of the velocity are presented. Comparison with experiment is discussed.

TABLE OF CONTENTS

LIST OF ILLUSTRATIONS

I. INTRODUCTION

The unsteady motion of a fluid which fills a spinning right-circular cylinder is considered in this paper. The spin is imparted impulsively to the cylinder and the spin-up of the fluid is perturbed to study the wave motion in the rotating fluid. This is called the spin-up eigenvalue problem; abbreviated e.v. problem. Because of boundary layers and the critical layer that exist in the flow, the problem is formulated with viscous perturbations. The physical significance of the critical layer is discussed as well as how it affects the solution of the numerical problem. The term "critical layer" is used here because it is analogous to the critical layer that occurs in the Orr-Sommerfeld equation governing stability of a laminar shear layer; although the stability of the rotating flow is not a question here, the formulation of the e.v. problem is mathematically the same as for the stability problem. For the Orr-Sommerfeld equation, a critical layer exists if the disturbance phase velocity is equal to the basic flow shear velocity. For the rotating fluid, the condition for a critical layer is that the wave frequency be an integral multiple of the local angular frequency of the basic circumferential flow.

The application of this work is to the study of the flight of liquid-filled projectiles; these have a proclivity for unusual flight behavior, often being unstable even though the same projectile with a solid payload is stable. A knowledge of the wave motion in the rotating fluid is fundamental to an understanding of the effect of the liquid on the projectile motion.

The frequencies and decay rates of the waves are determined by the complex eigenvalues of the system of perturbation equations. For large time the fluid approaches solid body rotation; for this state there is no critical layer and the eigenvalue problem is considerably simpler. The critical layer always exists for small time; it ceases to exist at a time which depends on the parameters of the basic flow and the wave motion.

The physics of the basic flow, spin-up from rest, was presented by Wedemeyer.[1] The flow is determined by Reynolds number = Re = $\Omega a^2/\nu$ and aspect ratio = A = c/a where Ω is the spin (rad/ sec), a and c are the radius and half-height of the cylinder and ν is the kinematic viscosity of the fluid. The model determines the core flow, not that in the endwall boundary layers. The flow can also be determined in a more complete way by solving the Navier-Stokes equations by finite difference methods. For the e.v. problem it would be impractical to use the finite difference solution for the basic flow.

A discussion of previous attempts to solve the e.v. problem is given in Reference 2 together with more details of the work presented here. Experimental data such as velocity fields, pressures, or gyroscopic motion of the

---

1. *E. H. Wedemeyer, "The Unsteady Flow Within a Spinning Cylinder," Journal of Fluid Mechanics, Vol. 20, Part 3, 1964, pp. 383-399. (See also BRL Report No. 1225, October 1963, AD 431846.)*

2. *R. Sedney and N. Gerber, "Oscillations of a Liquid in a Rotating Cylinder: Part II. Spin-Up," US Army Ballistic Research Laboratory, Aberdeen Proving Ground, MD, BRL Technical Report ARBRL-TR-02489, May 1983. (AD A129094)*

container exist for the range of parameters $1 < Re < 10^7$ and $1 \leq A \leq 5$. The spin-up basic flow and the e.v. analyses are restricted to the higher Re by virtue of some asymptotic approximations. The lower bound on Re for applicability of the e.v. results is not known, in general. For axisymmetric perturbations it appears to be $O(10^2)$; see Reference 3. At present the analysis of the rotating fluid problem, per se, is also limited because the boundary layers on the cylinder endwalls, i.e., the Ekman layers, and the Stewartson layer on the sidewall are not included. For application to the projectile problem the angular motion must be restricted to small angles because the theory is linearized.

Whether or not the effects of the time dependent, spin-up basic flow are important in a projectile flight, rather than solid body rotation of the fluid, can be estimated by comparing the characteristic time for spin-up, $\tilde{t}_s$, with the time of flight of the projectile. If the former is small compared to the latter, spin-up effects can be neglected. For laminar Ekman layers,

$$\tilde{t}_s = (2c/a)\ Re^{1/2}/\Omega = 2/E^{1/2}\ \Omega \qquad \text{(sec)}$$

where $E = \nu/\Omega c^2$ is the Ekman number, often used in rotating fluid problems rather than Re. This estimate is derivable from linear spin-up theory[4,5] or the Wedemeyer model. We use the non-dimensional characteristic spin-up time $t_s = \Omega \tilde{t}_s$. For $Re > 10^5$, approximately, the Ekman layers may be turbulent, in which case the characteristic spin-up time can be estimated by

$$\tilde{t}_{st} = (28.6\ c/a)\ Re^{1/5}/\Omega \qquad \text{(sec)}$$

which can be obtained from the Wedemeyer solution without diffusion for turbulent Ekman layers.[1] These times do not measure how close the flow is to solid body rotation. A rule of thumb often used, but not always accurate, is that solid body rotation is reached at about $4\tilde{t}_s$ after an impulsive angular velocity is applied to the cylinder.

To appreciate these time scales for projectile applications, consider two cases which will be used to present illustrative numerical results:

---

3. *R. Sedney, N. Gerber, and J. M. Bartos, "Oscillations of a Liquid in a Rotating Cylinder," AIAA 20th Aerospace Sciences Meeting, January 11-14, 1982, Orlando, Florida, AIAA Paper 82-0296. (See also ARBRL-TR-02488, May 1983, AD A129088.)*

4. *H. P. Greenspan, The Theory of Rotating Fluids, Cambridge University Press, London and New York, 1968.*

5. *E. R. Benton and A. Clark, Jr., "Spin-Up," article in Annual Review of Fluid Mechanics, Vol. 6, Annual Reviews, Inc., Palo Alto, CA, 1974.*

	Re	c/a	Ω (rad/sec)	$\bar{t}_s$ (sec)
Case 1:	4,974	3.30	8937	0.052
Case 2:	1.99×10^6	5.20	754	3.510

These parameters, courtesy of Dr. W. P. D'Amico, are appropriate, for Case 1, to a test of small caliber projectiles in a ballistic range, and for Case 2 to an artillery projectile. At the spin-up times the projectiles would be 48 m and 1,230 m from the gun for Cases 1 and 2, respectively; in both cases observations on projectile motion could be made at these distances. Partial validation of the theory has been provided by experiments[6] and numerical simulations.[3]

Some of the first part of this report repeats what is in Reference 2. It is included here for convenience.

II. THE SPIN-UP BASIC FLOW

Consider the axisymmetric, time dependent motion of a fluid which fills a cylinder, initially at rest, which is impulsively brought to a constant angular velocity Ω with respect to its axis. In practice, an impulsive start is impossible; the conditions for approximating it and the degree of approximation in some experimental apparatus and in a gun tube are discussed in Reference 7. For an impulsive start, the validity of the Wedemeyer model can be discussed in terms of three time scales: the time for one revolution of the cylinder, $2\pi\Omega^{-1}$, $\bar{t}_s$ or $\bar{t}_{st}$, and the time for vorticity to diffuse radially, Re Ω^{-1}. The model requires $2\pi\Omega^{-1} \ll \bar{t}_s \ll \mathrm{Re}\,\Omega^{-1}$.

It is known that the Ekman layers form and become essentially steady in time $2\pi\Omega^{-1}$. Although Wedemeyer[1] showed the crucial importance of the Ekman layers to the spin-up process, his model did not require a solution for the flow in these layers; exclusion of this solution has important consequences for the e.v. problem. The basic mechanism for spin-up starts with the suction exerted by the Ekman layers which draws external fluid into them where rotation is induced. With no pressure gradient acting, the fluid spirals out to larger radii where the layers eject fluid. At those radii the flow outside the Ekman layers, called the core flow, is now rotating. This mechanism is

---

6. *S. Stergiopoulos, "An Experimental Study of Inertial Waves in a Fluid Contained in a Rotating Cylindrical Cavity During Spin-Up from Rest," Ph.D. Thesis, York University, Toronto, Ontario, February 1982.*

7. *R. Sedney and N. Gerber, "Viscous Effects in the Wedemeyer Model of Spin-Up From Rest," US Army Ballistic Research Laboratory, Aberdeen Proving Ground, MD., BRL Technical Report ARBRL-TR-02493, June 1983. (AD A129506)*

much more efficient than diffusion which plays a small role in spin-up. Wedemeyer[1] showed in his remarkable paper that the flow must be divided into two regions: the Ekman layers and the core flow. Actually an additional boundary layer, a Stewartson layer, is required at the side wall.

In the following, lengths, velocities, pressure, and time are made nondimensional by a, $a\Omega$, $\rho\Omega^2 a^2$, and Ω^{-1}, respectively, where ρ is the liquid density. In the inertial frame cylindrical coordinates, r, θ, z are used, with the origin of z at the center of the cylinder, and velocities are U, V W, respectively. Dimensionless time is t. Derivatives are indicated by subscripts.

Starting from the Navier-Stokes equations for axisymmetric flow Wedemeyer used order of magnitude arguments to simplify them in the core flow. The three momentum equations reduce to

$$V_t + U\,(V_r + V/r) = Re^{-1}\,[V_{rr} + (V/r)_r] \qquad (2.1)$$

and

$$U_z = V_z = P_z = 0 \qquad (2.2)$$

For $Re \to \infty$ he proposed neglecting the diffusion terms in (2.1) so that

$$V_{wt} + U_w\,(V_{wr} + V_w/r) = 0 \qquad (2.3)$$

where the subscript w indicates this approximation. Wedemeyer used (2.3) rather than (2.1) when he applied his model.

To solve (2.1), (2.3) a relationship between U and V is necessary. Wedemeyer used the facts that Ekman layers are steady after one revolution and that the radial mass flux in the core flow must be balanced by that in the Ekman layers to obtain some conditions on the U, V relationship. At this point he was forced to take a phenomenological approach. The relationship is known at $t \to 0$ and $t \to \infty$ and he proposed a linear interpolation between them to obtain an approximate relationship for any t. He tested this idea in some other problems where the solution was known and decided it was satisfactory. Some confusion has appeared in later literature because this step was misinterpreted; this matter is discussed in Reference 7. The result is

$$U = k_\ell(V-r) \qquad k_\ell = \kappa(a/c)Re^{-1/2} = 2\kappa/t_s \qquad (2.4)$$

for laminar Ekman layers. Wedemeyer proposed $\kappa = 0.443$ but Greenspan[4] suggested $\kappa = 0.5$; the latter often gives results in better agreement with numerical solutions to the Navier-Stokes equations. Other relationships have been proposed, but they will not be discussed here; see Reference 7. For turbulent Ekman layers

$$U = -k_t(r-V)^{8/5} \qquad k_t = 0.035(a/c)Re^{-1/5} = 1/t_{st} \qquad (2.5)$$

where t_{st} is the nondimensional, turbulent spin-up time. The core flow is assumed to be laminar so that turbulent stresses are not introduced in the right-hand side of (2.1).

Using (2.4), (2.3) can be solved explicitly:

$$V_w = (r\, e^{2k_\ell t} - 1/r)/(e^{2k_\ell t} - 1) \quad \text{for } r > e^{-k_\ell t} \qquad (2.6)$$

and $V_w = 0$ otherwise. Therefore, $r = r_f = e^{-k_\ell t}$ separates rotating and nonrotating fluid where there is a discontinuity in shear. W is obtained from the continuity equation: $W = -(z/r)\ (rU)_r$. At $r = 1$, $W \neq 0$; thus, the Stewartson layer should be included at $r = 1$, but this has yet to be done. Also $W \neq 0$ at the end walls $z = \pm c/a$.

Wedemeyer pointed out that the corner in the solution (2.6) would be smoothed out if the diffusion terms were retained, as in (2.1). But this is a nonlinear second order equation and must be integrated by finite difference methods. This can be done with some standard techniques for diffusion equations. Special treatment is needed near the point $r = 1$, $t = 0$ because, for an impulsive start, a discontinuity in the boundary conditions exists at that point. In our work a local, analytic solution was derived to resolve the discontinuity; see Reference 8. In most of our e.v. calculations we used the V from the numerical solution of (2.1) with either (2.4) or (2.5), but other options are also used. For laminar Ekman layers, the spin-up velocity profile

$$V = f\ (r,\ k_\ell t,\ k_\ell\ Re);$$

for the turbulent case k_ℓ is replaced by k_t.

Some examples of the solutions of (2.1) will be given to illustrate the V profiles which must be perturbed in the e.v. problem. The parameters of Cases 1 and 2 are used in V(r,t) presented in Figure 1. For Case 1, the relation

---

8. R. Sedney and N. Gerber, "Treatment of the Discontinuity in the Spin-Up Problem with Impulsive Start," US Army Ballistic Research Laboratory, Aberdeen Proving Ground, MD., BRL Technical Report ARBRL-TR-02520, September 1983. (AD A133682)

for laminar Ekman layers, (2.4), is used and for Case 2, (2.5) is used. For each case the results for three times are shown. As $t \to +0$, V tends to a discontinuous function; for small t, an asymptotic solution to (2.1) was derived in Reference 8 using erf functions. The e.v. analysis uses a quasi-steady assumption which is violated as $t \to +0$. A practical limit on how small t should be in the analysis is set by the smallest t at which data can be obtained.

III. THE PERTURBED FLOW

The procedure for obtaining the equations governing the perturbed flow is a standard one and will only be outlined. The velocity components and pressure, expressed as the sum of the spin-up basic flow and the perturbation, e.g., $U^*(r,z,t) + u'(r, \theta,z,t)$, are substituted into the Navier-Stokes equations for 3-D, unsteady flow. Initially the basic flow, e.g., U^*, is a solution to the Navier-Stokes equations for axisymmetric flow, the zeroth order terms. The first order terms, linear in the perturbations, are retained and the second order terms are neglected. The coefficients in the linear perturbation equations are the basic flow variables and their derivatives. The basic flow is now approximated by the results from the Wedemeyer model. All coefficients containing U^* and W^* and their derivatives with respect to r and z are $O(1/t_s)$ - except one term discussed below; all those containing V^* are $O(1)$. Replacing V^* by V, the resulting perturbation equations contain only V, not U and W; they are

$$u'_t+(V/r)u'_\theta-2Vv'/r = -p'_r+Re^{-1}(\nabla^2u'-u'/r^2-2v'_\theta/r^2)$$

$$v'_t+[V_r+(V/r)]u'+(V/r)v'_\theta = -p'_\theta/r+Re^{-1}(\nabla^2v' - v'/r^2+2u'_\theta/r^2 \qquad (3.1)$$

$$w'_t+(V/r)w'_\theta = -p'_z+Re^{-1}\nabla^2w'$$

$$(ru')_r+v'_\theta+ rw'_z = 0.$$

These equations govern viscous perturbations of the core flow. If a formal, rational expansion with $Re^{-1/2}$ as the parameter had been used the viscous or Re^{-1} terms would not appear. These govern the inviscid perturbations and are adequate except in the perturbation boundary layer and the critical layer. The viscous terms could be included by local analyses in these two regions. We have included them in a global sense by retaining the Re^{-1} terms. In the derivation of (3.1), one term in the z-momentum equations contains W^*_r. If this is approximated by W_r that term is not small near $r = 1$ because the Wedemeyer model requires a Stewartson layer there, as discussed earlier. Therefore, strictly, (3.1) are valid outside the Stewartson layer; this restriction does not appear to be a serious one.

Finally, employing the quasi-steady assumption in (3.1) is considered. The time scale for the perturbation is $O(1)$; that for V is $O(t_s)$ where $t_s >> 1$, except for $t \to +0$ as discussed earlier. With that exception the variation of V with t in (3.1) is slow and t can be regarded as a parameter in $V(r,t)$.

IV. THE EIGENVALUE PROBEM

A. The Mathematical Model.

It is convenient to introduce the new coordinate $z' = z + A$. It is assumed that the perturbation can be represented as a superposition of modes. With the quasi-steady assumption such a separation of variables is possible. In complex notation

$$u' = \text{Real}\left\{u(r) \cos Kz' \exp\left[i(Ct-m\theta)\right]\right\} \tag{4.1}$$

with similar expressions for v' and p'; w' has the same form except for a $\sin Kz'$ factor. Here $K = k\pi/2A$ with $k = 1,2,...$ and $m = 0, \pm 1,...$the axial and azimuthal wave numbers, respectively; $m = 1$ is the value relevant to the projectile problem. The complex quantities u,v,w,p are solutions of the system of ordinary differential equations obtained by substituting the modal forms into (3.1). The nondimensional complex constant

$$C = C_R + i\,C_I$$

is the eigenvalue of the system. The dimensional wave frequency is $C_R\Omega$ and the decay rate is $C_I\Omega$.

For the free oscillation problem the boundary conditions at the end walls $z' = 0$, $2A$ are $u' = v' = w' = 0$ if the complete flow is being perturbed. Since we are perturbing the core flow, not the Ekman layers, the boundary conditions are not the same. The modal forms give $w' = 0$ but u' and v' do not satisfy the no-slip condition. Appropriate inner expansions in the Ekman layers are required to correct this. Here the modal form is used without end-wall correction. The modal form is also used for the solid rotation case for which there are no Ekman layers. However, endwall corrections are still necessary; the perturbation boundary layer must be introduced. Not including this correction gives values of C_I which are incorrect by a factor of 2 but the effect on C_R is about 1%. An ad hoc method of including an endwall correction for the spin-up case is to use the solid rotation correction for finite time. This ad hoc correction is advantageous for large t.

From (3.1) a sixth order system of ordinary differential equations is obtained:

$$[Re^{-1}(\Delta_1 - r^{-2}) - i\ M]u + (2/r)(V + i\ m\ r^{-1}Re^{-1})v - p_r = 0$$

$$[Re^{-1}(\Delta_1 - r^{-2}) - i\ M]v - (\partial V/\partial r + V/r + 2i\ m\ Re^{-1}/r^2)u + i\ m\ p/r = 0 \qquad (4.2)$$

$$[Re^{-1}\Delta_1 - i\ M]\ w + K\ p = 0$$

$$(r\ u)_r - i\ m\ v + K\ r\ w = 0.$$

where

$$\Delta_1 f \equiv f_{rr} + f_r/r - [(m^2/r^2) + K^2]f$$

and

$$M(r) = C - mV/r \qquad (4.3)$$

The no-slip boundary conditions at $r = 1$ require

$$u = v = w = 0 \qquad \text{at } r = 1. \qquad (4.4)$$

The boundary conditions at $r = 0$ depend on m; they are derived using continuity and single-valuedness. For $m = 1$

$$u - iv = w = p = 0 \qquad \text{at } r = 0. \qquad (4.5)$$

The system (4.2), (4.4), and (4.5) is not self-adjoint. Although there is no proof, we assume the e.v. form a denumerable, discrete spectrum. With index n used to order the spectrum, the e.v. are C_n. The system must be solved for C_n and the eigenfunctions u_n, v_n, w_n, p_n given V, c/a, Re, m and k; t enters only through V. If the system were self-adjoint the index n would be the radial mode number. For this non-self-adjoint system it is unclear how to define a mode in a general and unambiguous manner. A mode can be identified for large t by calculating the e.v. for $t \to \infty$, where the radial mode number is known for the solid rotation solution, and then tracked as t decreases. This identification is unambiguous if the critical layer does not exist.

B. The Numerical Method.

For V (r;t) obtained from the finite difference solution to (2.1), the system (4.2), (4.4) and (4.5) must be integrated for $0 \leq r \leq 1$. The numerical method used to solve the e.v. problem is a shooting method with iteration. The numerical integration cannot start at r = 0 because (4.2) have a singularity there. Three regular linearly independent solutions were obtained that satisfy (4.5) for m = 1 using power series expansions near r = 0 and expressing V as a power series in r. These solutions, evaluated at $r = \varepsilon$, are used as initial conditions for the numerical integration of (4.2) for $\varepsilon \leq r \leq 1$; typically $\varepsilon = .001$. Further details are given in Reference 2.

Integration of (4.2) is not straightforward because the coefficient of the highest order derivative, Re^{-1}, is small for the values of Re of interest. To insure that the linearly independent solutions remain so as the integration proceeds, orthonormalization was applied; a modification of Davey's technique[9] was used; see Reference 10 for details. Typically, orthonormalization was applied at 50 equally-spaced points with an integration interval of .001; these parameters are varied depending on the case considered.

Before the integration process is started a value of C must be specified, the first guess for C_n. A linear combination of the 3 linearly independent solutions is tested to see if (4.4) is satisfied. This test requires that the characteristic determinent Z(C) = 0. If $Z \neq 0$ within a certain tolerance, a new value of C is obtained using Newton's method; Muller's method has also been used. Equation (4.2) is integrated again with the new value of C, etc. The iteration continues until a convergence test on the iterates is satisfied. The e.v. is then known and the constants in the linear combination are determined to give the eigenfunctions. One of these constants is set equal to unity for convenience, which normalizes the eigenfunctions.

Usually a spin-up e.v. history is required. The computation is started at large t where the first guess can be obtained from the C_n for solid body rotation or the inviscid approximation to it. For smaller t the first guess is obtained by extrapolation. As t decreases this first guess may not be sufficiently close to the desired e.v. and the iteration process will either converge to some other e.v. or diverge; a more detailed searching process is then required. In our computations of C_n this has occurred for n = 2 and

---

9. *A. Davey, "A Simple Numerical Method for Solving Orr-Sommerfeld Problems," Quarterly Journal of Mathematics and Applied Mechanics, Vol. 26, Part 4, 1973, pp. 401-411.*

10. *C. W. Kitchens, Jr., N. Gerber, and R. Sedney, "Oscillations of a Liquid in a Rotating Cylinder: Part I. Solid-Body Rotation," US Army Ballistic Research Laboratory, Aberdeen Proving Ground, MD., BRL Technical Report ARBRL-TR-02081, June 1978. (AD A057759)*

small t in which case the solution of the e.v. problem becomes more laborious. The need for a more detailed search is indicated by the shape of the surfaces Z(C) and will be illustrated by an example.

For Case 1, sections of the surfaces Z(C) will be shown for C in the neighborhood of C_2, at t = 155. For illustrative purposes it is convenient to plot the single surface $|Z|(C_R, C_I)$ but only sections of that surface with planes C_I = constant are shown in Figure 2. For the parameters of Case 1, m = 1, k = 3 and t = 155, C_{R2} = .072614 and C_{I2} = .034266. The shape of the surface changes rapidly in the neighborhood of that point for small changes in C_R and C_I. The first guess must be in an interval ΔC_R = .0005 and ΔC_I = .0003 about the e.v., that is within about 1% of C_2; otherwise the iteration converged to C_1. The high peak near the zero of $|Z|$ is symptomatic of this behavior. A method for handling this situation was developed. Note that, for n = 1, but all other parameters the same as above, the $|Z|$ vs C_R curves are monotonic on either side of the e.v. and the first guess can be chosen in a much larger interval; in fact extrapolation is sufficient.

The time to calculate one C depends on many parameters. For straightforward cases, typical CPU times for one C calculation are 1 minute on the CDC 7600 and 5 minutes on the VAX.

V. THE CRITICAL LAYER

The Orr-Sommerfeld equation that governs the perturbations on a 2-D shear flow can be regarded as a prototype for the system (4.2). The former is 4th-order rather than 6th-order and there is no singularity at the origin in the O-S case. However, the stiff nature of the O-S equation, because of the Re^{-1} factor, and the possible existence of a critical layer make it a useful guide in the present problem. A recent review of various aspects of the critical layer in the O-S case was given by Stewartson.[11] A discussion of it using the classical solutions to the O-S equation can be found in Schlichting[12] together with a description of the famous Schubauer and Skramstad experiment which verified the change in phase of the streamwise component of velocity across the critical layer. The change in phase of the Reynolds stress across the critical layer is essential to an understanding of the instability of a shear flow.

The definition of the critical layer is best appreciated by considering the inviscid perturbation equations. In the limit Re → ∞ the O-S equation reduces to the Rayleigh equations for inviscid disturbances. For a neutral

---

11. *K. Stewartson, "Marginally Stable Inviscid Flows with Critical Layers," Journal of Applied Mathematics, Vol. 27, 1981, pp. 133-175.*

12. *H. Schlichting, Boundary Layer Theory, 4th Edition, McGraw-Hill Book Company, New York, 1960, Chapter XVI.*

disturbance, if there is a point at which the phase velocity is equal to the basic flow shear velocity (and the curvature there is not zero), this point is called a critical level and its neighborhood the critical layer. The critical level is a singular point of the Rayleigh equation; a discontinuity in the perturbation velocity is implied, violating the small disturbance assumption. There are ways of circumventing the singular behavior.[11] For the O-S equation the critical level is a turning point but not a singular point. Some of the effects of the critical layer are different for amplifying and decaying disturbances. The latter are analogous to the effects in the present work.

The inviscid limit of the perturbation equations for the rotating fluid case is obtained by setting $Re^{-1} = 0$ in (4.2). The order of the system is reduced from six to two and this system is analogous to the Rayleigh equations. Consider a neutral disturbance, i.e., $C_I = 0$. The coefficient of the highest order derivative contains $M = C - mV/r$ and the C is real. If $M = 0$ has a real root, r_c, where $0 < r_c < 1$, the equation has a singular point at the critical level r_c and the small disturbance assumption is violated. The neighborhood of r_c is called the critical layer. The physical interpretation of

$$C_R = mV/r \tag{5.1}$$

at $r = r_c$ is that the wave frequency is an integral multiple of the angular frequency of the basic-flow, indicating a resonance. If $m = 0$ or if m and C_R have opposite signs there is no critical layer. The nature of the V vs r curves shown in Figure 1 shows that an r_c always exists for small t if $m \neq 0$ and $\operatorname{sgn} m = \operatorname{sgn} C_R$ but will not exist for large t. There can be a critical layer for each n.

For viscous perturbations (4.2) do not have a singularity when $M = 0$. The r for which $M = 0$, in general complex, is a turning point of (4.2). However, the neighborhood of real r_c obtained from (5.1) is still called the critical layer. One practical consequence of the existence of the critical layer is that the eigenfunctions can develop high frequency oscillations of large relative amplitude. These occur, most notably, for small t and large Re. The integration scheme and the number of significant figures in the computation must be capable of resolving these in order to get a solution to the e.v. problem for (4.2).

Lynn[13] showed that the thickness of the critical layer is $O(Re^{-1/3})$ as it is in the O-S case. The critical layer and the boundary layer, $O(Re^{-1/2})$, can merge at the lower Re. Stewartson[11] showed, analytically, for the O-S case,

---

13. *Y.M. Lynn, "Free Oscillations of a Liquid During Spin-Up," US Army Ballistic Research Laboratory, Aberdeen Proving Ground, Maryland, ARBRL Report No. 1663, August 1973. (AD A769710)*

that the interval over which the eigenfunctions are "violently oscillatory" is proportional to C_I for a given basic shear flow; this could not be verified by the results for the rotating fluid case.

VI. RESULTS

Some results for eigenfunctions, e.v., and the critical layer will be shown. It is convenient to designate the three wave numbers by the triplet (k, n, m) corresponding to the wave numbers for the (z, r, θ) directions.

Table 1. Effect of Neglecting Diffusion.

WITH DIFFUSION				WITHOUT DIFFUSION			
t	C_R	$C_I \times 10^3$	r_c	C_R	$C_I \times 10^3$	r_c	r_f
600	.149	17.1	.423	.232	27.2	.668	.618
1245	.0855	3.14	----	.132	4.44	.392	.368

In Figure 3 the eigenfunction Real (w) = w_R vs r is shown at three times for Re = 5×10^5, A = 2.679, t_s = 3,788 and mode (5,1,1); laminar Ekman layers are assumed. In Figure 3a, t = 7,000, t/t_s = 1.85, $C_R = 8.354 \times 10^{-2}$, $C_I = 8.363 \times 10^{-4}$ and there is no critical layer; the variation of w_R through the boundary layer can be barely discerned on this scale. In Figure 3b, t = 1000, t/t_s = .26, $C_R = 7.060 \times 10^{-2}$, and r_c = 0.44 as indicated by the arrow in the figure; the rapid variation of w_R in the neighborhood of r_c is typical of the effects of the critical layer on the eigenfunctions for Re > 10^4, approximately. In Figure 3c, t = 400, t/t_s = .11, $C_R = 3.015 \times 10^{-2}$, $C_I = 8.066 \times 10^{-2}$, and r_c = 0.66; outside the critical layer w_R is not zero although it appears to be on this scale. The oscillations of w_R are centered at $r = r_c$. The max $|w_R|$ is greater in Figure 3c compared to that of Figure 3a by a factor of 1900. For the conditions of Figure 3c, if Ω = 628 rad/sec (100 Hz), $\bar{t}$ = 0.64 sec.

Time histories for C_1 and C_2 are shown in Figure 4 for Case 1 and modes (3,1,1) and (3,2,1). The C_{R1} curve has a shallow maximum and minimum for 180 $< t < 220$ but on the scale of this figure it appears to be constant. At t = 45 it has a maximum which is typical for all C_{R1} vs t curves; note that $C_R = 0$ for $t = 0$. The signficance of a maximum in the C_{R1} curve is related to a necessary condition for projectile instability. If the nutational frequency is less than the maximum of C_R, there are two times at which instability might develop. The C_{I1} and C_{R2} curves are rather typical, but the C_{I2} curve is not because it has a maximum at $t = 195$ and an inflection point at $t = 170$; these make it difficult to obtain a first guess for C_2. The problems encountered in calculating C_2 for $t \leq 200$ were discussed in Section IV-2. Since $C_{I2} < C_{I1}$ for $t<140$ the $n = 2$ mode could be more significant than the $n = 1$ mode for projectile instability.

The variation of r_c with t is shown in Figure 5 for both Cases 1 and 2 and $n = 1$ and 2. Note the two time scales. For both cases r_c=0 at an earlier time for $n = 1$. The r_c's for $n = 1$ and 2 are equal when $C_{R1} = C_{R2}$ but $C_{I1} \neq C_{I2}$ and the eigenfunctions are distinct. For Case 1, $n = 1$, $r_c = 0$ at $t = 225 = .489\ t_s$ and for Case 2, $n = 1$, $r_c = 0$ at $t = 9950 = 3.76\ t_{st}$ which gives $\bar{t}$ = 13.2 sec. Thus for Case 2 the critical layer exists over a substantial part of the projectile flight time; however, its effects are not great when r_c is small.

As a digression from the presentation of results, consider the implications of using (2.3), which neglects diffusion terms, to determine the basic flow V profiles. Its solution is (2.6) for $r \geq r_f$ and zero otherwise. In Table 1 the e.v. and r_c determined this way are compared with those using the V including diffusion for Re = 39,771, A = 3.12, t_s = 1,245, mode (3,1,1) and $\kappa = 0.5$. Neglecting diffusion gives large errors in C and r_c and the r_c is never zero except in the limit $t \to \infty$.

The C_R time history for Case 2, mode (5,1,1) using the turbulent Ekman layer compatibility condition (2.5) is given in Figure 6; the maximum occurs for $t < 1,200$. Calculations for this case and some related ones were used to plan projectile firings and then to analyze the results in Reference 14. In

14. *W.P. D'Amico, Jr., "Flight Data on Liquid-Filled Shell for Spin-Up Instabilities," US Ballistic Research Laboratory, Aberdeen Proving Ground, Maryland, BRL Memorandum Report ARBRL-MR-03334, February 1984. (See also AIAA Paper 83-2143, August 1983.)*

planning such tests the sensitivity of C_R to variations of parameters must be considered. The results for two such variations are shown in Figure 6: Re was decreased by a factor of 10 keeping A fixed which decreased C_R and A was increased by 10% keeping Re fixed which increased C_R; the relative changes vary with t. In the first variation Re is in the transition range; turbulent Ekman layers were assumed. There is a large change in $r_c(t)$ for the first variation, e.g., $r_c = 0$ at $t = 3200$ compared to 9950 for Case 2. For the second variation $r_c(t)$ does not differ much from Case 2, e.g., $r_c = 0$ at $t = 11{,}700$. The spin-up times are 1671 and 2912 for the first and second variations, respectively.

The rapid change in phase of the velocity across the critical layer in the O-S case was mentioned earlier. In the rotating fluid case the change in phase of u' for $0 \leq r < 1$ will be shown. From (4.1)

$$u' = (u_R^2 + u_I^2)^{1/2} e^{-C_I t} \times \cos Kz' \sin [\beta - (C_R t - m\theta)] \tag{6.1}$$

$$\tan \beta = -u_R/u_I \ .$$

The phase angle $\beta(r)$ is plotted in Figure 7 for Case 2. The rapid change in phase in the critical layer is evident for t = 2000, 6000, and 9000; the magnitude of the phase change in the critical layer is approximately 223°, 180°, and 180°, respectively. Another rapid change in β takes place in the sidewall boundary layer. This phase angle change is a sensitive indication of the critical layer. As t increases, the r interval over which β is essentially constant increases. For the conditions of Figure 7, β = constant, except in the boundary layer, for $t \geq 10{,}000$ for which $r_c = 0$.

The wave surface u' = constant can be obtained from (6.1). For fixed z' and t this surface appears as a curve in the (r,θ) plane. For certain values of the parameters, the variation with r of $(u_R^2 + u_I^2)^{1/2}$ can be neglected and the wave surface is given, approximately, by

$$\theta = \text{constant} - \beta(r)$$

This curve is plotted in Figure 8 for Case 2, n = 1 at t = 6,000. If there were no boundary layer or critical layer, the curve would be a straight line through the origin.

For n = 2 the $\beta(r)$ curves include a phase change across the critical layer, as for n = 1, and that arising from the fact that u_R and u_I must each have a zero since the radial mode number has increased by one. In Figure 9 $\beta(r)$ is shown for Case 2, n = 2 at t = 6,000 for which $r_c = .303$. The total change in phase for $0 \leq r \leq 1$ is about 400°, considerably larger than that for

$n = 1$ shown in Figure 7. (That this is not always the case is shown by the next example.) In addition to those in the critical layer, u_R and u_I have zeros at $r = .420$ and $.503$, respectively. For no critical layer, say $t = 16{,}000$, there is an abrupt change in phase of 180°, rather than a constant β as for $n = 1$.

The slopes of the $\beta(r)$ curves in the critical layer are not as large for smaller Re. In Figure 10 $\beta(r)$ is plotted for Case 1 at $t = 160$ for $n = 1, 2$ for which $r_c = .304, .176$, respectively. Here the change in phase for $n = 2$ is less than that for $n = 1$.

VII. DISCUSSION

The theory and a method for the solution of the spin-up e.v. problem were presented here. The theory for the perturbed flow is a linear one but not for the basic flow. Because viscous effects are important in the boundary layer at the cylinder wall and in the critical layer, viscous perturbations are used. The theory has limitations because of the various assumptions that are made. The theory and method are successful in the sense that they provide results that are physically meaningful and do not violate intuition or the "physics of the problem." Other investigators have worked on this problem without success in that sense. The more important gauge of success is validation by comparison with either experimental results or numerical simulation.

For the solid rotation case and $m = 0$, a detailed validation was given in Reference 3 using numerical simulation. This provides confidence in the treatment of (4.2), and the solid rotation endwall correction, for that case. Spin-up and $m = 0$ could be validated in the same way; it would require, relatively, more analysis to reduce the numerical data. At the present time there is no numerical simulation to validate the $m = 1$ case.

To the authors' knowledge, the only reported measurements of C for $m = 1$ are in Reference 6. Some experimental results for C_R vs t, using the methods of Reference 6, are shown in Figure 11; Stergiopoulos, private communication. The fact that the data are in groups of 3 points, is an artifact of the data reduction process. For each group Re = constant; for all groups $4.39 \leq \mathrm{Re} \times 10^{-4} \leq 4.45$, a negligible variation. The aspect ratio $A = 0.600$ and the mode is (1,2,1). The scatter in the data is about ±3% except at $t=245$ where it is ±5%. The calculated C_R, using $\kappa = 0.443$, is within the scatter of data. This comparison validates the calculation of C_R for these parameters over the range of the data $0.724 \leq t/t_s \leq 2.252$. For large t, essentially at solid rotation, the experimental and calculated results differ by 1.5%.[6] The $r_c(t)$ curve shows that the critical layer exists over a considerable range for which data is presented.

The percent differences of C_R, the frequency with respect to an inertial frame, are considerably larger than those for the frequency with respect to the rotating frame, C_{Rr}. For solid rotation, or steady state, it is more

conventional to work in the rotating frame.[4] The relationships between the two frequencies and their percentage changes are

$$C_R = 1 - C_{Rr}$$

$$\Delta C_R/C_R = -(\Delta C_{Rr}/C_{Rr})\ (1 - C_R)/C_R$$

Comparisons of experimental and calculated C_R for modes (2,1,0) and (1,1,1,) give the same conclusions as for the (1,2,1). Comparisons of C_I are not shown for two reasons: (i) the experimental error in the determination of C_I can be quite large and (ii) not accounting for the Ekman layers in the calculation gives C_I's about one-half of the proper values; the effect on C_R is 1 - 2%.

There are no data in the spin-up range from projectile firings that can be used to validate this theory. Some indirect, qualitative results are given in Reference 14 which show consistency with the theory presented here. Further validation will probably depend on laboratory experiments.

ACKNOWLEDGMENT

The authors wish to thank Ms. Joan M. Bartos for her work on a large number of tasks which made the programs used here operational. Her programming and editing were essential to the completion of this work.

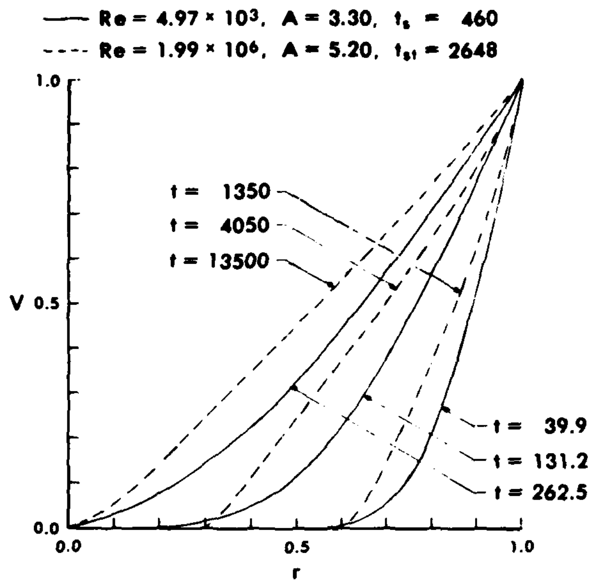

Figure 1. V vs r for Cases 1 and 2 at Three Times; κ = 0.5.

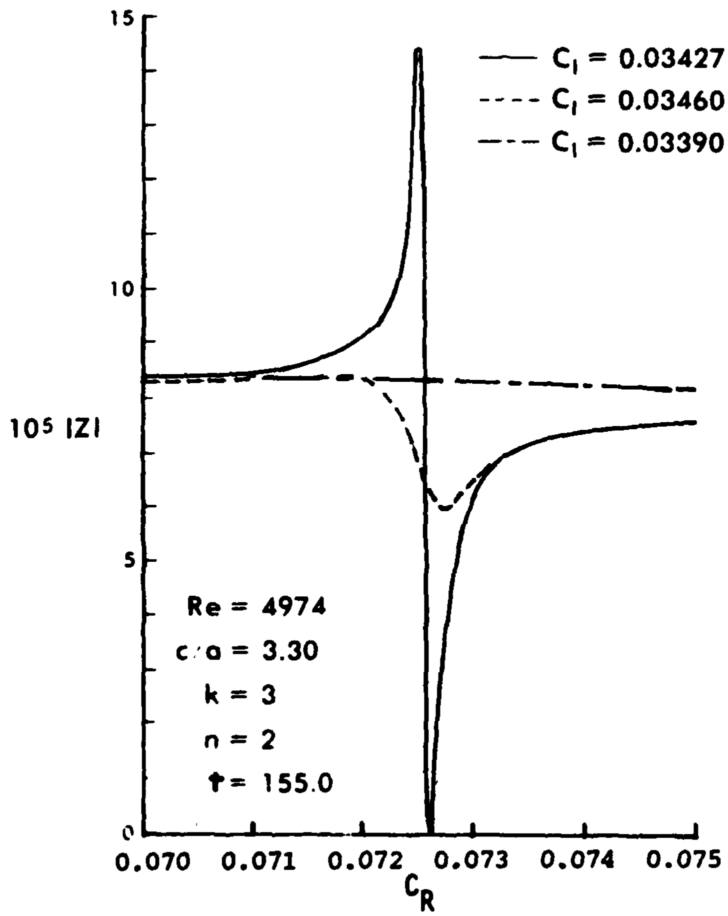

Figure 2. The Magnitude of the Characteristic Determinant, $|Z|$, vs C_R for Three Values of C_I for Case 1, m = 1, k = 3, t = 155. C_{R2} = .072614, C_{I2} = .034266.

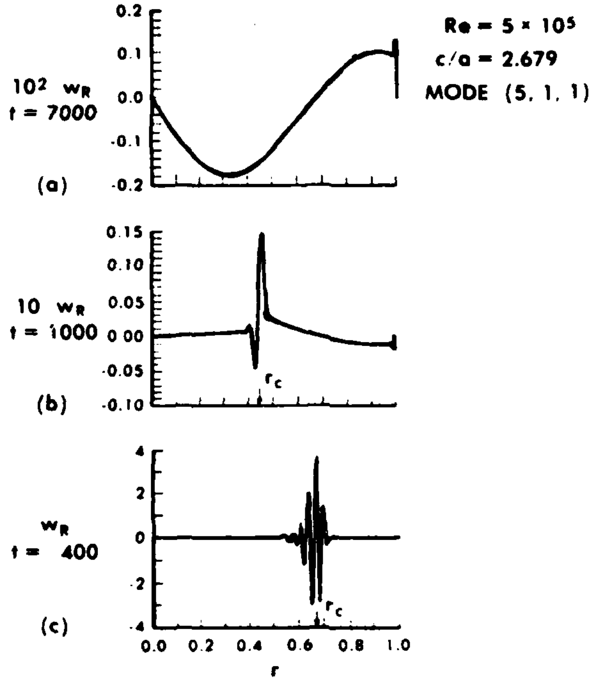

Figure 3. The Eigenfunction Real (w) vs r for Re = 5 x 10^5, A = 2.679, Mode (5,1,1), t_s = 3788. Note Scale Changes.

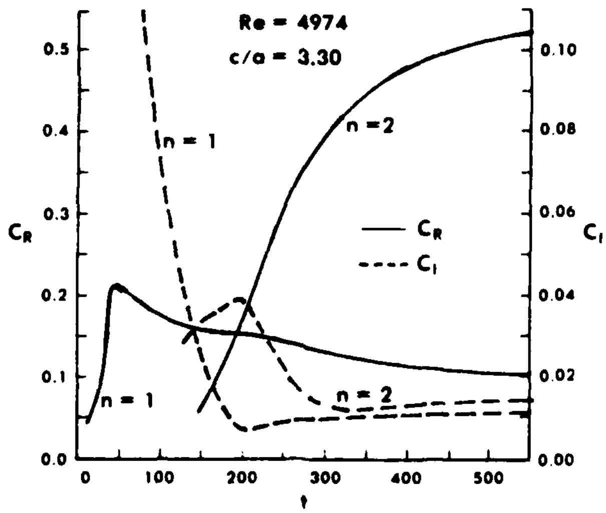

Figure 4. Time Histories for C_1 and C_2 for Case 1, Modes (3,1,1) and (3,2,1), t_s = 460, κ = 0.5.

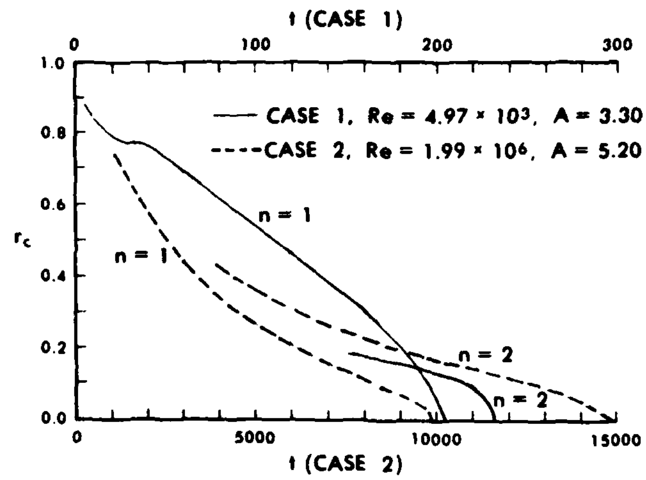

Figure 5. Critical Level, r_c, vs t for Cases 1 and 2, n = 1 and 2, κ = 0.5.

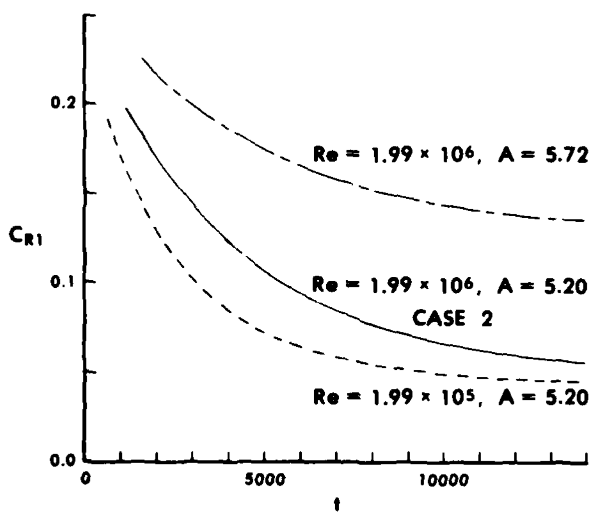

Figure 6. C_{R1} vs t for Case 2, Mode (5,1,1) and for Two Variations on Case 2.

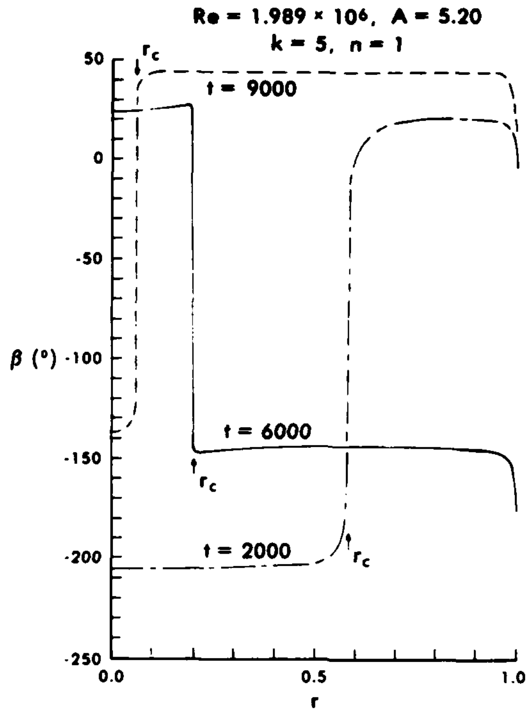

Figure 7. The Phase Angle of u' for Case 2, Mode (5,1,1) at Three Times.

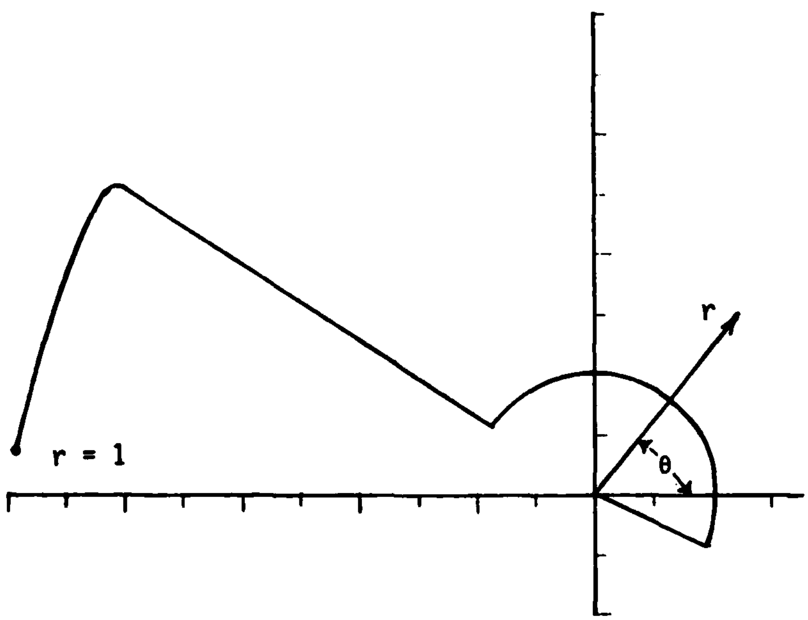

Figure 8. In the (r,θ) Plane, the Approximate Wave Surface u' = Constant for Fixed z' and t for Case 2, Mode (5,1,1) at t = 6,000. The Circular Arc Portion Is at the Critical Level $r = r_c = .20$; the Change in θ Near r = 1 Occurs in the Boundary Layer.

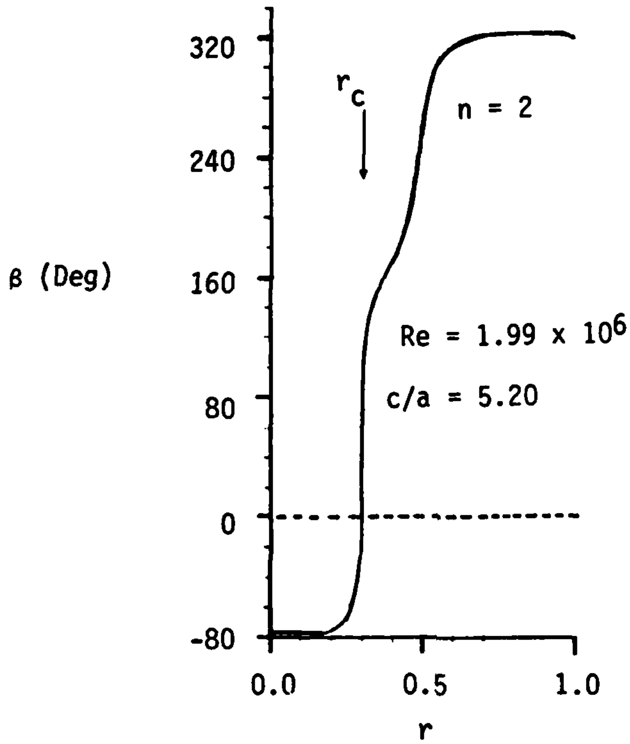

Figure 9. The Phase Angle of u' for Case 2, Mode (5,2,1) at t = 6,000. The Critical Level is at r_c = .303.

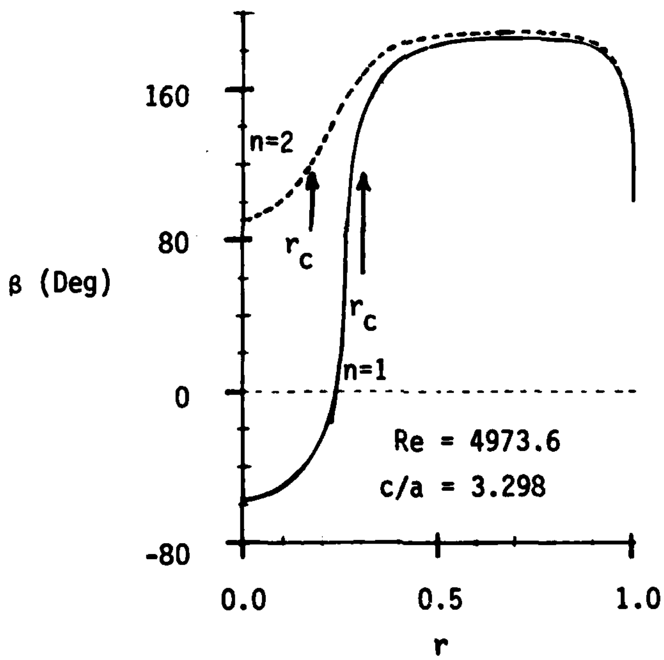

Figure 10. The Phase Angle of u' for Case 1, Modes (3,1,1) and (3,2,1) at t = 160.

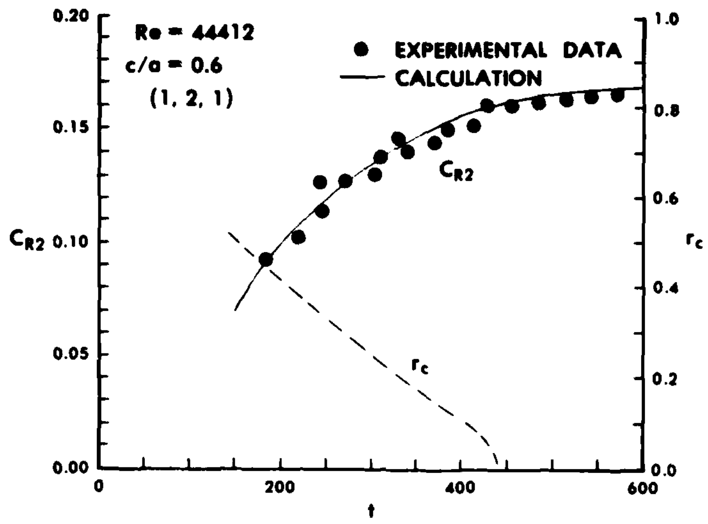

Figure 11. C_R vs t: Experimental Points and Calculated Values; r_c vs t, $\kappa = 0.443$.

REFERENCES

1. E. H. Wedemeyer, "The Unsteady Flow Within a Spinning Cylinder," Journal of Fluid Mechanics, Vol. 20, Part 3, 1964, pp. 383-399. (See also BRL Report No. 1225, October 1963, AD 431846.)

2. R. Sedney and N. Gerber, "Oscillations of a Liquid in a Rotating Cylinder: Part II. Spin-Up," US Army Ballistic Research Laboratory, Aberdeen Proving Ground, Maryland, BRL Technical Report ARBRL-TR-02489, May 1983. (AD A129094).

3. R. Sedney, N. Gerber, and J. M. Bartos, "Oscillations of a Liquid in a Rotating Cylinder," AIAA 20th Aerospace Sciences Meeting, January 11-14, 1982, Orlando, Florida, AIAA Paper 82-0296. (See also ARBRL-TR-02488, May 1983. AD A129088.)

4. H. P. Greenspan, The Theory of Rotating Fluids, Cambridge University Press, London and New York, 1968.

5. E. R. Benton and A. Clark, Jr., "Spin-Up," article in Annual Review of Fluid Mechanics, Vol. 6, Annual Reviews, Inc., Palo Alto, CA, 1974.

6. S. Stergiopoulos, "An Experimental Study of Inertial Waves in a Fluid Contained in a Rotating Cylindrical Cavity During Spin-Up from Rest," Ph.D. Thesis, York University, Toronto, Ontario, February 1982.

7. R. Sedney and N. Gerber, "Viscous Effects in the Wedemeyer Model of Spin-Up From Rest," US Army Ballistic Research Laboratory, Aberdeen Proving Ground, Maryland, BRL Technical Report ARBRL-TR-02493, June 1983. (AD A129506)

8. R. Sedney and N. Gerber, "Treatment of the Discontinuity in the Spin-Up Problem with Impulsive Start," US Army Ballistic Research Laboratory, Aberdeen Proving Ground, Maryland, BRL Technical Report ARBRL-TR-02520, September 1983. (AD A133682)

9. A. Davey, "A Simple Numerical Method for Solving Orr-Sommerfeld Problems," Quarterly Journal of Mathematics and Applied Mechanics, Vol. 26, Part 4, 1973, pp. 401-411.

10. C. W. Kitchens, Jr., N. Gerber, and R. Sedney, "Oscillations of a Liquid in a Rotating Cylinder: Part I. Solid-Body Rotation," US Army Ballistic Research Laboratory, Aberdeen Proving Ground, Maryland, BRL Technical Report ARBRL-TR-02081, June 1978. (AD A057759)

11. K. Stewartson, "Marginally Stable Inviscid Flows with Critical Layers," Journal of Applied Mathematics, Vol. 27, 1981, pp. 133-175.

12. H. Schlichting, Boundary Layer Theory, 4th Edition, McGraw-Hill Book Company, New York, 1960, Chapter XVI.

13. Y. M. Lynn, "Free Oscillations of a Liquid During Spin-Up," US Army Ballistic Research Laboratory, Aberdeen Proving Ground, Maryland, BRL Report No. 1663, August 1973. (AD A769710)

14. W. P. D'Amico, Jr., "Flight Data on Liquid-Filled Shell for Spin-Up Instabilities," US Army Ballistic Research Laboratory, Aberdeen Proving Ground, Maryland, BRL Memorandum Report ARBRL-MR-03334, February 1984, (AD A139136). (See also AIAA Paper 83-2143, August 1983.)

DISTRIBUTION LIST

No. of Copies	Organization
12	Administrator Defense Technical Information Center ATTN: DTIC-DDA Cameron Station Alexandria, VA 22314
1	Commander US Army Engineer Waterways Experiment Station P.O. Box 631 ATTN: R. H. Malter Vicksburg, MS 39180
1	Commander US Army Materiel Development and Readiness Command ATTN: DRCDRA-ST 5001 Eisenhower Avenue Alexandria, VA 22333
1	Commander Armament R&D Center US Army AMCCOM ATTN: DRSMC-TDC(D) Dover, NJ 07801
1	Commander Armament R&D Center US Army AMCCOM ATTN: DRSMC-TSS(D) Dover, NJ 07801
6	Commander Armament R&D Center US Army AMCCOM ATTN: DRSMC-LCA-F(D) Mr. D. Mertz Mr. E. Falkowski Mr. A. Loeb Mr. R. Kline Mr. S. Kahn Mr. S. Wasserman Dover, NJ 07801
1	Commander US army Development & Employment Agency ATTN: MODE-TED-SAB Ft. Lewis, WA 98433
1	Commander US Army Armament Munitions and Chemical Command ATTN: DRSMC-LEP-L(R) Rock Island, IL 61299
1	Director Benet Weapons Laboratory Armament R&D Center US Army AMCCOM ATTN: DRSMC-LCB-TL(D) Watervliet, NY 12189
1	Commander US Army Aviation Research and Development Command ATTN: DRDAV-E 4300 Goodfellow Blvd St. Louis, MO 63120
1	Director US Army Air Mobility Research and Development Laboratory ATTN: SAVDL-D, W.J. McCroskey Ames Research Center Moffett Field, CA 94035
1	Commander US Army Communications Research and Development Command ATTN: DRSEL-ATDD Fort Monmouth, NJ 07703
1	Commander US Army Communications Rsch and Development Command ATTN: DRSEL-L Fort Monmouth, NJ 07703
1	Commander US Army Electronics Research and Development Command Technical Support Activity ATTN: DELSD-L Fort Monmouth, NJ 07703
1	HQDA DAMA-ART-M Washington, DC 20310

DISTRIBUTION LIST

No. of Copies	Organization
1	Commander US Army Missile Command ATTN: DRSMI-YDL Redstone Arsenal, AL 35898
1	Commander US Army Missile Command ATTN: DRSMI-R Redstone Arsenal, AL 35898
1	Commander US Army Missile Command ATTN: DRSMI-RDK, Mr. R. Deep Redstone Arsenal, AL 35898
1	Commander US Army Tank Automotive Command ATTN: DRSTA-TSL Warren, MI 48090
1	Director US Army TRADOC Systems Analysis Activity ATTN: ATAA-SL White Sands Missile Range, NM 88002
1	Commander US Army Jefferson Proving Grd Madison, IN 47250
2	Commander US Army Research Office ATTN: Dr. R.E. Singleton Dr. Jagdish Chandra P.O. Box 12211 Research Triangle Park, NC 27709
1	AGARD-NATO ATTN: R.H. Korkegi APO New York 09777
1	AFWL/SUL Kirtland AFB, NM 87117

No. of Copies	Organization
1	Commandant US Army Infantry School ATTN: ATSH-CD-CSO-OR Fort Benning, GA 31905
3	Commander Naval Air Systems Command ATTN: AIR-604 Washington, DC 20360
2	Commander David W. Taylor Naval Ship Research & Development Ctr ATTN: H.J. Lugt, Code 1802 S. de los Santos Bethesda, MD 20084
1	Commander Naval Surface Weapons Center ATTN: DX-21, Lib Br Dahlgren, VA 22448
4	Commander Naval Surface Weapons Center Applied Aerodynamics Division ATTN: J.T. Frasier M. Ciment A.E. Winklemann W.C. Ragsdale Silver Spring, MD 20910
1	AFATL (DLDL, Dr. D.C.Daniel) Eglin AFB, FL 32542
2	AFWAL (W.L. Hankey; J.S. Shang) Wright-Patterson AFB, OH 45433
1	Aerospace Corporation Aero-Engineering Subdivision ATTN: Walter F. Reddall El Segundo, CA 90245
1	Commander US Army Development & Employment Agency ATTN: MODE-TED-SAB Fort Lewis, WA 98433

DISTRIBUTION LIST

No. of Copies	Organization
5	Director National Aeronautics and Space Administration Ames Research Center ATTN: D.R. Chapman J. Rakich W.C. Rose B. Wick P. Kutler Moffett Field, CA 94035
2	Director National Aeronautics and Space Administration Langley Research Center ATTN: Tech Library J. South Langley Station Hampton, VA 23365
1	Director National Aeronautics and Space Administration Lewis Research Center ATTN: MS 60-3, Tech Lib 21000 Brookpark Road Cleveland, OH 44135
2	Director National Aeronautics and Space Administration Marshall Space Flight Center ATTN: A.R. Felix, Chief S&E-AERO-AE Dr. W.W. Fowlis Huntsville, AL 35812
3	Aerospace Corporation ATTN: H. Mirels R.L. Varwig Aerophysics Lab. P.O. Box 92957 Los Angeles, CA 90009
2	Director Jet Propulsion Laboratory ATTN: L.M. Mach Tech Library 4800 Oak Grove Drive Pasadena, CA 91103
3	Arnold Research Org., Inc. ATTN: J.D. Whitfield R.K. Matthews J.C. Adams Arnold AFB, TN 37389
1	AVCO Systems Division ATTN: B. Reeves 201 Lowell Street Wilmington, MA 01887
3	Boeing Commercial Airplane Company ATTN: R.A. Day, MS 1W-82 P.E. Rubbert, MS 3N-19 J.D. McLean, MS-3N-19 Seattle, WA 98124
3	Calspan Corporation ATTN: G. Homicz P.O. Box 400 Buffalo, NY 14225
1	General Dynamics ATTN: Research Lib 2246 P.O. Box 748 Fort Worth, TX 76101
1	General Electric Company, RESD ATTN: W.J. East 3198 Chestnut Street Philadelphia, PA 19101
2	Grumman Aerospace Corporation ATTN: R.E. Melnik L.G. Kaufman Bethpage, NY 11714

DISTRIBUTION LIST

No. of Copies	Organization
2	Lockheed-Georgia Company ATTN: B.H. Little, Jr. G.A. Pounds Dept 72074, Zone 403 86 South Cobb Drive Marietta, GA 30062
1	Lockheed Missiles and Space Company ATTN: Tech Info Center 3251 Hanover Street Palo Alto, CA 94304
3	Martin-Marietta Corporation ATTN: S.H. Maslen S.C. Traugott H. Obremski 1450 S. Rolling Road Baltimore, MD 21227
2	McDonnell Douglas Astronautics Corporation ATTN: J. Xerikos H. Tang 5301 Bolsa Avenue Huntington Beach, CA 92647
1	McDonnell-Douglas Corporation Douglas Aircraft Company ATTN: T. Cebeci 3855 Lakewood Boulevard Long Beach, CA 90801
3	Rockwell International Science Center ATTN: Dr. V. Shankar Dr. N. Malmuth Dr. S. Chakravarthy 1049 Camino Dos Rios Thousand Oaks, CA 91360
4	Sandia National Laboratory ATTN: H.W. Vaughn F.G. Blottner W.L. Oberkampf Tech Lib. Albuquerque, NM 87115
2	United Aircraft Corporation Research Laboratory ATTN: M.J. Werle; Library 400 Main Street East Hartford, CT 06108
1	Vought Systems Division LTV Aerospace Corporation ATTN: J.M. Cooksey, Chief, Gas Dynamics Lab, 2-53700 P.O. Box 5907 Dallas, TX 75222
1	Arizona State University Department of Mechanical and Energy Systems Engineering ATTN: G.P. Neitzel Tempe, AZ 85281
1	Cornell University Graduate School of Aero Engr ATTN: Library Ithaca, NY 14850
3	California Institute of Technology ATTN: Tech Library H.B. Keller, Math Dept D. Coles, Aero Dept Pasadena, CA 91109
1	Illinois Institute of Tech ATTN: H. M. Nagib 3300 South Federal Chicago, IL 60616
1	The Johns Hopkins University Dept of Mech and Materials Sci. ATTN: S. Corrsin Baltimore, MD 21218
1	Louisiana State University Dept. of Physics and Astronomy ATTN: Dr. R.G. Hussey Baton Rouge, LA 70803

DISTRIBUTION LIST

No. of Copies	Organization
4	Director Johns Hopkins University Applied Physics Laboratory ATTN: Dr. R.D. Whiting Dr. D.A. Hurdif Dr. R.S. Hirsh Mr. E.R. Bohn Johns Hopkins Road Laurel, MD 20707
3	Massachusetts Institute of Technology ATTN: E. Covert H. Greenspan Tech Lib 77 Massachusetts Avenue Cambridge, MA 02139
2	North Carolina State Univ Mechanical and Aerospace Engineering Department ATTN: F.F. DeJarnette J.C. Williams Raleigh, NC 27607
1	Northwestern University Department of Engineering Science and Applied Mathematics ATTN: Dr. S.H. Davis Evanston, IL 60201
1	Notre Dame University Department of Aero Engr ATTN: T.J. Mueller South Bend, IN 46556
2	Ohio State University Dept of Aeronautical and Astronautical Engineering ATTN: S.L. Petrie O.R. Burggraf Columbus, OH 43210
2	Polytechnic Institute of New York ATTN: G. Moretti S.G. Rubin Route 110 Farmingdale, NY 11735
3	Princeton University James Forrestal Research Ctr Gas Dynamics Laboratory ATTN: S.M. Bogdonoff S.I. Cheng Tech Library Princeton, NJ 08540
1	Purdue University Thermal Science & Prop Ctr ATTN: Tech Library W. Lafayette, IN 47907
1	Rensselaer Polytechnic Institute Department of Math Sciences ATTN: R.C. Di Prima Troy, NY 12181
1	Southern Methodist University Department of Civil and Mechanical Engineering ATTN: R. L. Simpson Dallas, TX 75272
1	San Diego State University Department of Aerospace Engr and Engineering Mechanics College of Engineering ATTN: K.C. Wang San Diego, CA 92182

DISTRIBUTION LIST

No. of Copies	Organization
1	Southwest Research Institute Applied Mechanics Reviews 8500 Culebra Road San Antonio, TX 78228
2	Stanford University Dept of Aeronautics/Astronautics ATTN: Dr. J.L. Steger Dr. S. Chakravarthy Stanford, CA 94305
1	Texas A&M University College of Engineering ATTN: R.H. Page College Station, TX 77843
1	University of California - Davis ATTN: H.A. Dwyer Davis, CA 95616
1	University of California - Berkeley Department of Aerospace Engineering ATTN: M. Holt Berkeley, CA 94720
2	University of California - San Diego Department of Aerospace Engineering and Mechanical Engineering Sciences ATTN: P. Libby Tech Library La Jolla, CA 92037
1	University of Cincinnati Department of Aerospace Engineering ATTN: R.T. Davis Cincinnati, OH 45221
1	University of Colorado Department of Astro-Geophysics ATTN: E.R. Benton Boulder, CO 80302

No. of Copies	Organization
2	University of Maryland ATTN: W. Melnik J.D. Anderson College Park, MD 20740
1	University of Maryland - Baltimore County Department of Mathematics ATTN: Dr. Y.M. Lynn 5401 Wilkens Avenue Baltimore, MD 21228
1	University of Santa Clara Department of Physics ATTN: R. Greeley Santa Clara, CA 95053
2	University of Southern California Department of Aerospace Engineering ATTN: T. Maxworthy P. Weidman Los Angeles, CA 90007
2	University of Michigan Department of Aeronautical Engineering ATTN: W.W. Wilmarth Tech Library East Engineering Building Ann Arbor, MI 48104
2	University of Rochester Department of Mechanical and Aerospace Sciences ATTN: R. Gans A. Clark, Jr. Rochester, NY 14627
1	University of Tennessee Department of Physics ATTN: Prof. W.E. Scott Knoxville, TN 37916

DISTRIBUTION LIST

No. of Copies	Organization
1	University of Texas Department of Aerospace Engineering ATTN: J.C. Westkaemper Austin, TX 78712
1	University of Virginia Department of Aerospace Engineering & Engineering Physics ATTN: I.D. Jacobson Charlottesville, VA 22904
1	University of Virginia Research Laboratories for the Engineering Sciences ATTN: Prof. H. G. Wood P.O. Box 3366 University Station Charlottesville, VA 22904
1	University of Washington Department of Mechanical Engineering ATTN: Tech Library Seattle, WA 98105
1	University of Wyoming ATTN: D.L. Boyer University Station Laramie, WY 82071
1	U.S. Military Academy Department of Physics ATTN: MAJ G. Heuser West Point, NY 10996
1	Woods Hole Oceanographic Institute ATTN: J.A. Whitehead Woods Hole, MA 02543
3	Virginia Polytechnic Institute and State University Department of Aerospace Engineering ATTN: Tech Library Dr. W. Saric Dr. T. Herbert Blacksburg, VA 24061

Aberdeen Proving Ground

Director, USAMSAA
ATTN: DRXSY-D
DRXSY-MP, H. Cohen

Commander, USATECOM
ATTN: DRSTE-TO-F

Commander, CRDC, USAAMCCOM
ATTN: DRSMC-CLN
W. C. Dee
DRSMC-CLB-PA
M. C. Miller
DRSMC-CLJ-L
DRSMC-CLB-PA
DRSMC-CLN

USER EVALUATION SHEET/CHANGE OF ADDRESS

This Laboratory undertakes a continuing effort to improve the quality of the reports it publishes. Your comments/answers to the items/questions below will aid us in our efforts.

1. BRL Report Number____________________ Date of Report__________

2. Date Report Received______________________________

3. Does this report satisfy a need? (Comment on purpose, related project, or other area of interest for which the report will be used.)__________

4. How specifically, is the report being used? (Information source, design data, procedure, source of ideas, etc.)__________

5. Has the information in this report led to any quantitative savings as far as man-hours or dollars saved, operating costs avoided or efficiencies achieved, etc? If so, please elaborate.__________

6. General Comments. What do you think should be changed to improve future reports? (Indicate changes to organization, technical content, format, etc.)

CURRENT ADDRESS

Name

Organization

Address

City, State, Zip

7. If indicating a Change of Address or Address Correction, please provide the New or Correct Address in Block 6 above and the Old or Incorrect address below.

OLD ADDRESS

Name

Organization

Address

City, State, Zip

(Remove this sheet along the perforation, fold as indicated, staple or tape closed, and mail.)

— — — — — — — — — — FOLD HERE — — — — — — — — — — —

Director
US Army Ballistic Research Laboratory
ATTN: DRXBR-OD-ST
Aberdeen Proving Ground, MD 21005-5066

NO POSTAGE
NECESSARY
IF MAILED
IN THE
UNITED STATES

OFFICIAL BUSINESS
PENALTY FOR PRIVATE USE, $300

BUSINESS REPLY MAIL
FIRST CLASS PERMIT NO 12062 WASHINGTON, DC

POSTAGE WILL BE PAID BY DEPARTMENT OF THE ARMY

Director
US Army Ballistic Research Laboratory
ATTN: DRXBR-OD-ST
Aberdeen Proving Ground, MD 21005-9989

— — — — — — — — — — FOLD HERE — — — — — — — — — — —

END

FILMED

10-84

DTIC